Light Metals 2012 *Edited by: Carlos E. Suarez*
TMS (The Minerals, Metals & Materials Society), 2012

Light Metals 2012

ALUMINUM ALLOYS: Fabrication, Characterization and Applications

ORGANIZERS
Subodh Das
Phinix, LLC
Lexington, Kentucky, USA

Zhengdong Long
Kaiser Aluminum
Spokane, Washington, USA

Tongguang Zhai
University of Kentucky
Lexington, Kentucky, USA

Light Metals 2012 *Edited by: Carlos E. Suarez*
TMS (The Minerals, Metals & Materials Society), 2012

Light Metals 2012

ALUMINUM ALLOYS: Fabrication, Characterization and Applications

Development and Application

SESSION CHAIR
Zhengdong Long
Kaiser Aluminum
Spokane, Washington, USA

Light Metals 2012 *Edited by: Carlos E. Suarez*
TMS (The Minerals, Metals & Materials Society), 2012

Precipitation of the $\theta'(Al_2Cu)$ phase in Al-Cu-Ag alloys

Julian M. Rosalie[1], Laure Bourgeois[2,3,4], Barrington C. Muddle[3,4]

[1]NIMS (National Institute for Materials Science), Sengen, Tsukuba, Ibaraki, 305-0047, Japan.
[2]MCEM, Monash University, Vic, 3800, Australia.
[3]Dept. of Materials Engineering, Vic, 3800, Australia.
[4] ARC Centre of Excellence for Design in Light Metals, Vic, 3800, Australia.

Keywords: Aluminium alloys, Precipitation, Nucleation

Abstract

Precipitation of the θ' (Al_2Cu) phase was examined in Al-(1.75-x) at.%Cu-x at.%Ag alloys. In alloys containing trace Ag the θ' precipitates formed T- or cross-shaped arrays of sympathetically-nucleated arrays similar to those reported in binary Al-Cu alloys. However, in alloys with equal atomic levels of copper and silver the θ' plates formed at specific sites on dislocation loops alongside pre-existing γ' ($AlAg_2$) precipitates. The dislocation loops appeared to dissociate at these sites in a manner which would provide a stacking fault that was isostructural with the θ' precipitate. Energy dispersive X-ray (EDX) mapping showed that the dislocation loops were silver-enriched at the sites where the θ' phase eventually precipitated and that a silver atmosphere remained after precipitation of the θ' plates.

Introduction

The binary Al-Cu system is one of classic alloy systems employed for fundamental studies of precipitation strengthening in alloys and solid-solid phase transformations in general. Of principle interest has been the precipitation of the body-centred tetragonal θ' (Al_2Cu) phase as plate-shaped precipitates with (100) habit. Nucleation of θ' precipitates can be stimulated through pre-ageing deformation and models have been developed to explain the precipitation of a single variant of the θ' precipitate on dislocations [1]. In the absence of external deformation, binary Al-Cu alloys develop a microstructure containing arrays of θ' precipitates stretching [2–5]. These arrays were thought to be formed through sympathetic nucleation, in which the volumetric strain field of one precipitate lowered the local strain energy barrier to nucleation of alternate variants of the phase. The resulting arrays appear highly ordered, with hundreds of precipitates maintaining a fine balance of strain.

Trace element additions have long been known to have a strong influence on θ' precipitation. Additions of Sn, In and Cd, for example stimulate the nucleation of the θ' phase, resulting in more accelerated isothermal ageing, a more refined precipitate distributions and subsequently greater strength [6–8]. These elements share high vacancy affinity and it is thought that solute-vacancy clusters acted as preferred sites for θ' nucleation. The exact mechanism by which various elements operate remains incomplete. Tin particles have been shown to adopt a different crystal structure when in contact with a θ' precipitate [9], suggesting a more complex interaction that simply the provision of excess vacancies.

There were a number of early studies on Al-Ag-Cu alloys, although silver did not appear to exert as significant an influence on the precipitation of the θ' phase. X-ray studies noted that for compositions of around 1at.%Cu, 1at%Ag, isothermal ageing resulted in the precipitation of both θ' (Al_2Cu) precipitates on the {100} planes and a silver-containing phase, γ' ($AlAg_2$) on {111} planes [10]. It was noted that this composition contained a higher number density of precipitates. A recent study on Al-0.90at.%Ag-0.90at%Cu noted that θ' precipitates did not form arrays in this alloy [11]. Instead the precipitates appeared to have a close association with γ' precipitates which had formed on dislocation loops. However, no further details of θ' phase precipitation in this alloy have been described.

Experimental Details

The alloy compositions used were of the form Al-1.75-x at.%Cu-x at.%Ag in order to investigate the effect of 1:1 replacement of Cu by Ag in the well-studied Al-1.75at.%Cu alloy (Al-4.0wt.%Cu) alloy. Compositions selected were x=0 (binary Al-Cu), x=0.08 and x=0.90. The ternary compositions were chosen so as to contrast the effect of trace and moderately high levels of Ag on θ' phase precipitation and are described hereafter as AlCu(Ag) and AlCuAg.

All alloys were were cast in air at 700°C into graphite-coated steel molds, using high-purity Al (Cerac alloys, 99.99% purity), Cu (AMAC alloys, 99.99%) and Ag (AMAC alloys, 99.9+%). Ingot homogenised at 525°C for

7 days, then hot and cold-rolled to produce 0.5 mm sheet. Discs (3mm diameter, 0.5 mm thickness) were punched from the sheet. No further external deformation was applied after this point.

Inductively-coupled plasma atomic emission spectrometry (ICP-AES) yielded compositions for the AlAg(Cu) alloy Al-1.74at.%Ag-0.08at.%Ag (Al-4.00wt.%Cu-0.33wt.%Ag) and for AlAgCu: Al-0.90at.%Ag-0.90at.%Cu (Al-3.45wt.%Ag-2.05wt.%Cu).

Samples were solution treated for 0.5 h at 525°C in a nitrate/nitrite salt pot and quenched into water at ambient temperature. Rapid quenching from the solution-treatment temperature as found to be crucial and using the 0.5 mm thickness specimens assisted in maximising the cooling rate. Isothermal ageing was then conducted in an oil bath at 200°C for 0.16–2 h.

Samples were jet electropolished at -20°C using a nitric acid/methanol solution (33% HNO_3 / 67%CH_3OH v/v) to produce foils for TEM analysis. The applied voltages was typically around -13 V.

Diffraction contrast TEM images were obtained using a Phillips CM 20 microscope operating at 200 kV. High angle annular dark field (HAADF) scanning transmission electron microscope (STEM) images and energy dispersive X-ray (EDX) maps were obtained on a JEOL 2100F microscope operating at 200 kV with convergence semi-angle of 13 mrad and the inner and outer collection angles of 65 and 185 mrad respectively.

Results

The Al-Cu and AlCu(Ag) contained extended arrays of θ' precipitates similar to those previously reported in Al-Cu alloys. Fig. 1(a) shows the microstructure of the AlCu(Ag) alloy after 2 h ageing at 200°C. The figure shows a single arm of an array of precipitates, comprised of two variants of the θ' phase and extending well over 1μm. Such arrays were well-established following 1 h of ageing. The surrounding region is occupied by additional θ' precipitates which formed after the arrayed precipitates. The γ' phase was not observed in the AlAg(Cu) alloy.

The AlCuAg alloy contained no features of similar scale to the precipitate arrays. Fig. 1(b) shows a typical diffraction contrast TEM image of the microstructure of such an alloy, also aged for 2 h at 200°C. Instead of large arrays, γ' and θ' precipitates are clustered into structured assemblies comprised of around 5-10 precipitates. These assemblies were absent from the vicinity of vacancy sinks such as grain boundaries, as can be seen in the lower left of the figure. The inset in Fig. 1(b) shows a typical precipitate assembly in this alloy, containing two variants of γ' precipitates. θ' precipitates were observed after ageing times of at 2 h , by which time the γ' assemblies were well established. The θ' precipitates formed at sections of the assemblies tangential to (200) planes.

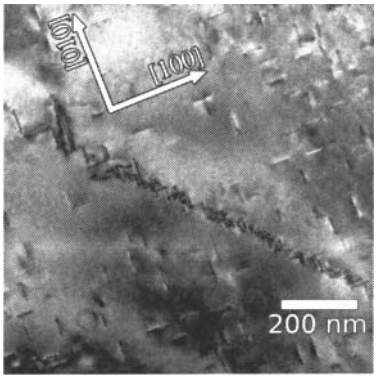

(a) Al-1.74at.%Cu-0.08at.%Ag.

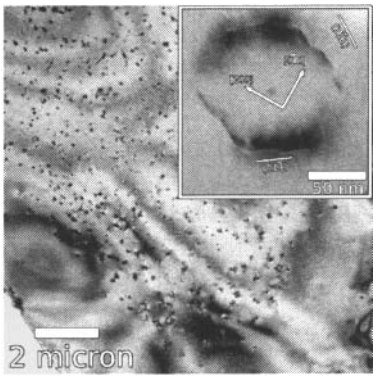

(b) Al-0.90at.%Cu-0.90at.%Ag.

Figure 1: A comparison of the microstructures of the AlCu(Ag) and AlCuAg alloys after 2 h ageing at 200°.

Fig. 2 shows two precipitate arrays normal to the [110] beam direction in a foil aged for 0.16 h. These arrays contain only γ' precipitates, with the regions tangential to (002) planes showing a diffuse strain contrast feature (labelled *A-D* in the figure). Fig. 2(b) presents a centred-dark field image taken with $\boldsymbol{g} = 0\bar{2}2$. The γ' precipitates are still visible, but the most notable feature is strong contrast at the sections of the assembly tangential to the (002) plane.

Fig. 3 shows a precipitate assembly in a foil aged for 2 h at 200°C. In the bright-field image (Fig. 3(a)) a single θ' precipitate (labelled *E*) can be seen to the upper right of the assembly.while the lower left corner (*F*) is devoid

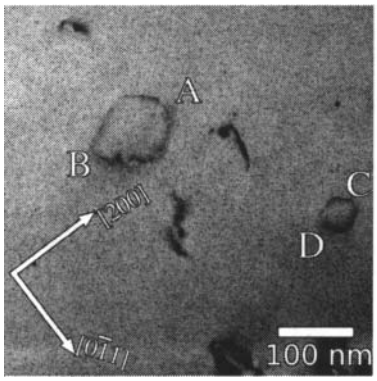

(a) Bright field°C. $\boldsymbol{g} = 0\bar{2}2$

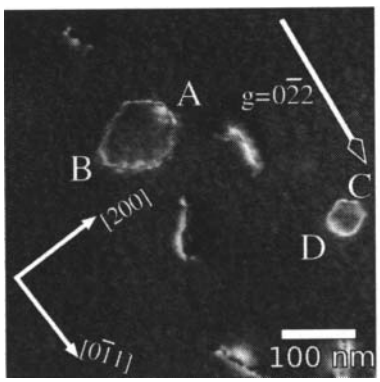

(b) Centred-dark field. $\boldsymbol{g}$=0$\bar{2}$2.

Figure 2: AlCuAg aged for 0.16 h at 200°C.

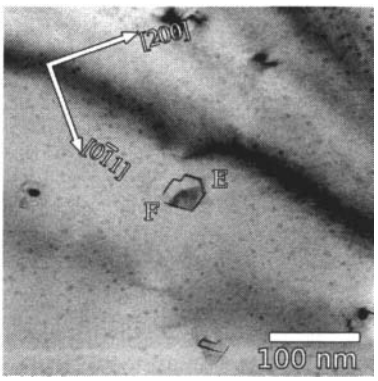

(a) Bright field.. $\boldsymbol{g}$=200.

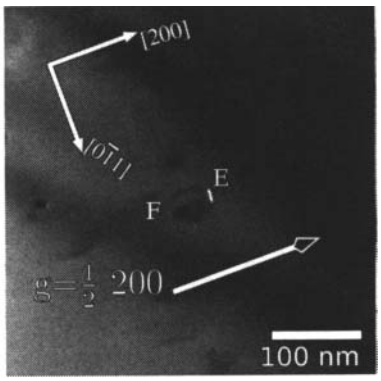

(b) Centred-dark field. $\boldsymbol{g} = \frac{1}{2}200$.

Figure 3: AlCuAg aged 2 h at 200°C.

of precipitates. A dark-field image (Fig. 3(b)) taken with $\boldsymbol{g} = \frac{1}{2}200$ shows strong contrast for the θ' precipitate, but no contrast enhancement at the opposite site of the assembly.

The microstructure of the AlCuAg alloy was examined in greater detail in order to clarify the reasons behind the change in precipitate morphology. Fig. 4(a) shows a bright field STEM image of a precipitate array containing only γ' precipitates in a foil aged for 0.5 h at 200°C. Aside from γ' precipitates with either $(1\bar{1}1)$ or $(11\bar{1})$ habit there is a diffuse contrast feature tangential to the (200) plane. This is shown in greater detail in the enlarged inset and takes the form of a diffuse double line with an overall width of 2 nm. The corresponding HAADF STEM image (Fig. 4(b)) shows strong atomic contrast in each of the γ' precipitates and in spherical GP zones surrounding the precipitate assembly. The defect line also shows enhanced contrast. At the convergence angles used the contrast is insensitive to strain, suggesting that this region is enriched in heavier elements relative to the surrounding matrix.

Energy dispersive X-ray maps for the framed regions in are given in Figures 4(c) and 4(d) indicate that this defect is enriched in silver, but not copper. The diffuse contrast feature is enriched in silver relative to the background. However there is no indication of additional copper along this defect. It should be noted that the overall copper content of the alloy is equal to the silver content and that the detection limits for the elements are not dissimilar. In addition, since a considerable amount of silver has partitioned to γ' precipitates the level of copper in solid solution will be greater than that of silver.

Fig. 5 shows a precipitate assembly in a foil aged for 2 h at 200°C. In the upper portion of the assembly a single θ' precipitate has formed, while in the lower portion of the field there is a diffuse contrast feature similar to that described in Fig. 4. Both bright field and Z-contrast images show much stronger contrast around the edges of the θ' precipitate. EDX maps for Cu and Ag (Figures 5(c), 5(d)) reveal Cu at the site of the θ' precipitate and Ag corresponding to the location of the γ' precipitates. Interestingly there is also enhanced silver around the θ' precipitate, which would appear to be responsible for the

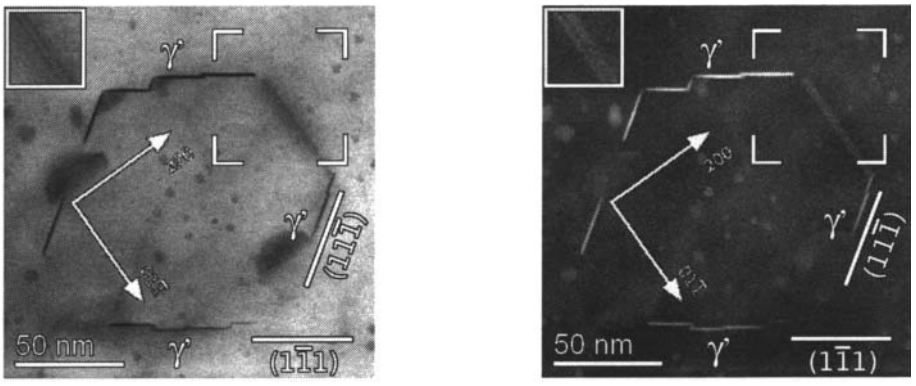

(a) Bright field STEM

(b) HAADF STEM

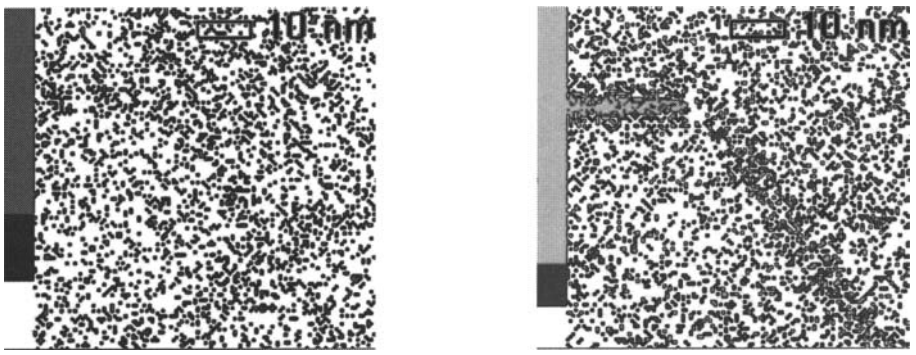

(c) Copper

(d) Silver

Figure 4: A γ' precipitate assembly. (a) and (b) shows bright field and HAADF STEM images of the region of interest with the diffuse contrast feature running from top left to bottom right. (c) and (d) shows an EDX map for the Cu K shell and Ag L shells, respectively.

contrast enhancement at the edges of the θ' precipitate, particularly in the Z-contrast image (Fig. 5(b)).

Discussion

Substitution of 0.90at.% silver for copper resulted in the θ' phase precipitating beside γ' precipitates in isolated assemblies, rather than in extended arrays. The change in precipitate morphology does not appear to be a trace element effect of the kind reported in several aluminium and magnesium alloy systems. The most well-studied example would be the addition of as little as 0.1at.%Ag to Al-Cu-Mg alloys which results in the precipitation of the Ω phase with {111} habit in place of θ'. In the present work at least 0.08.at%Ag could be substituted for Cu in Al-Cu alloys without substantially modifying the microstructure, as can be seen in Fig. 1(a).

The primary factor controlling the precipitate morphology appears to the level of copper in solution. Rapid quenching of pure Al results in the formation of Frank vacancy dislocation loops, but low-level Cu additions resulted in a gradual reduction of the dislocation loop size with increasing Cu content, and an eventual absence of loops altogether [12]. Cu is regarded as moderately strong vacancy-trapping element and develops substantial misfit strains in Al solid solution, so that vacancies are retained in association with the solute.

In contrast, silver additions have little impact on quenched-in defects in Al and up to 5.9at.% Ag can be added to pure Al without altering the nature of the dislocations loops [13]. Silver is unusual in that it does not generate appreciable misfit strains in Al solution, owing to its atomic size in solution begin near identical to that of the matrix. While consistent solute-vacancy binding energies are difficult to determine, silver is likewise generally regarded as a relatively weak-vacancy binding element.

In the AlCu(Ag) alloy the level of copper was sufficient to prevent dislocation loop formation, as would also be the case for the parent binary Al-Cu alloy. In this case the array morphology develops, whereby the volumetric strain due to precipitation of one θ' precipitate leads to a reduction in the strain energy barrier for nearby precipitation on alternate habit planes. For the AlCuAg alloy

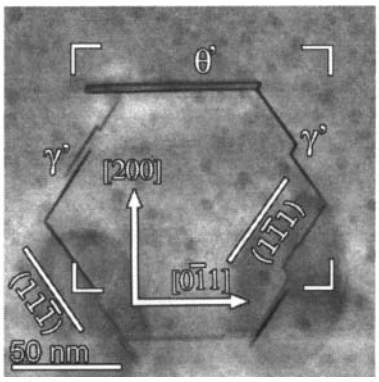

(a) Bright field STEM

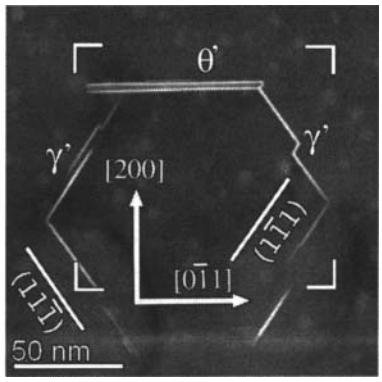

(b) HAADF STEM

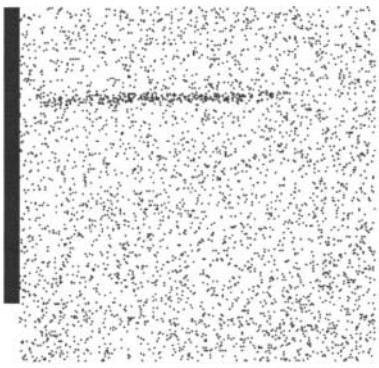

(c) Copper

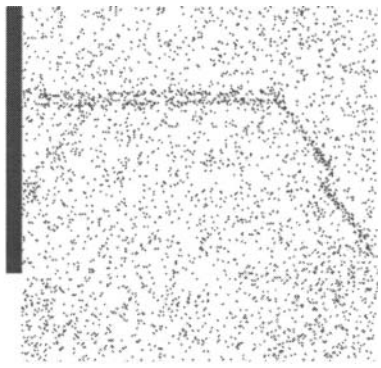

(d) Silver

Figure 5: A precipitate assembly containing a θ' precipitate. (a) and (b) show bright field and HAADF STEM images. (c) and (d) show EDX maps for the Cu K and Ag L shells, respectively.

there was insufficient copper to prevent dislocation loop formation. While this would not seem to preclude array formation, the complete absence of such arrays in all foils examined suggests that the dislocation loops offered a more favourable nucleation site.

The repeated precipitation of the θ' phase on dislocations [1] has been explained through the dissociation of the dislocation via the reaction [1]:

$$1/2\,[110] \rightarrow 1/2\,[100] + 1/2\,[010]$$

This process would lead to the generation of a single stacking fault on the (001) plane with body-centred tetragonal stacking. This layer would then be isostructural with the bct θ' precipitate and is therefore thought to facilitate the nucleation of the precipitate.

The dark-field images (Fig. 2) suggest that a similar process occurs within the dislocation loops. Perfect dislocation loops have edge character with a Burgers vector of type $\langle 011 \rangle$. For an assembly lying normal to the beam direction, therefore the electron beam is near-parallel to the Burgers vector and the dislocations have weak contrast (e.g. Figures 2(a),3(a),4(a)). Similar the contrast should be weak for both $\boldsymbol{g} = 200$ and $0\bar{2}2$ even when tilted a few degrees to a two-beam condition.

However, for a dissociated dislocation loop, with partials of type $\frac{1}{2}[100]$ and $\frac{1}{2}[010]$, the Burgers vector will be normal to $\boldsymbol{g} = 0\bar{2}2$ and strong contrast is expected, as is in Fig. 2(b). Conversely, for both partials, $\boldsymbol{g} \bullet \boldsymbol{B} = 0$ for $\boldsymbol{g} = \frac{1}{2}200$ and weak contrast is expected at the unoccupied end of the precipitate assembly (Fig. 3(b)). The diffraction contrast conditions for the relevant Burgers vector s and reflections are set out in Table I.

Precipitation of the γ' precipitates on dislocations and dislocation loops involves a similar process of dissociation to generate a stacking fault via the reaction:

$$1/2\,[110] \rightarrow 1/6\,[211] + 1/6\,[12\bar{1}]$$

Table I: Diffraction contrast conditions for edge dislocation loops on the (011) plane.

Defect	$\boldsymbol{b}$	$\boldsymbol{g}$	$\boldsymbol{b} \bullet \boldsymbol{g}$
Perfect loop	$\frac{1}{2}[011]$	200	0
		$0\bar{2}2$	0
Dissociated loop	$\frac{1}{2}[010]$, $\frac{1}{2}[001]$	200	0
		$0\bar{2}2$	± 1

This generates hcp stacking faults on either the $(\bar{1}11)$ or $(1\bar{1}1)$ planes [14–16], allowing for the nucleation of two variants of the γ' precipitate on a given dislocation loop [11].

Dissociation of a segment of the unit dislocation loop in this fashion would explain the formation of θ' precipitates at one (and later, frequently both) ends of the precipitate arrays. It is also consistent with the existence of only one variant of θ' on a given dislocation loop, since there is only one {100} plane on which the dislocation loop can dissociate to provide a isostructural surface.

It is not clear if Ag segregation plays a role in the precipitation of the θ' phase in AlAgCu. Given that there is no significant misfit strain for Ag in Al it does not appear to be a Cottrell atmosphere as usually defined. Computational studies have indicated a preference for Ag to cluster to {111} stacking faults due to the low stacking energy for Ag [17] , but it is not certain whether this would be the case for a stacking fault of different type on a different plane.

The vacancy content of the loops would allow rapid pipe diffusion around the dislocation loop. Under these conditions, entropic considerations would deem it particularly unfavourable for silver to be distributed around the dislocation loop except at the (200) tangents.

Fig. 5 indicates that a Ag atmosphere remains around the θ' precipitates. The presence of silver rather than copper at the defect where θ' precipitates later formed was a surprising observation. This is particularly interesting given that this silver atmosphere appears to persist around the θ' precipitates during the early stages of the latter's existence. It is not clear whether silver plays a direct role in θ' precipitation or growth and investigations into this question are underway.

Conclusions

Precipitation of the θ' (Al_2Cu) phase was examined in Al-Cu-Ag alloys. Substitution of trace levels of Ag did not substantially influence the precipitation of the θ' phase. When the level of Cu was insufficient to preclude dislocation loop formation the θ' phase formed on the dislocation loops beside previously-nucleated γ' precipitates. Sections of the dislocation loop tangential to {200} planes appear to dissociate in a way that would provide a faulted surface isostructural with the θ' phase, in a process analogous to the nucleation of θ' precipitates on perfect dislocations. X-ray mapping indicated that there was substantial segregation of silver to this region of the dislocation loop and that this persisted after the θ' phase had precipitated.

Acknowledgements The authors acknowledge use of the facilities at the Monash Centre for Electron Microscopy and engineering support by Russell King. JMR gratefully acknowledges the support of the Japan Society for the Promotion of Science (JSPS) through a JSPS fellowship.

References

[1] U. Dahmen, K. H. Westmacott, *Scripta Metall.*, **17**:(1983) 1241.

[2] V. Perovic, G. R. Purdy, *et al.*, *Acta Metall.*, **27**:(1979) 1075.

[3] V. Perovic, G. R. Purdy, *et al.*, *Scripta Metall.*, **14**(1):(1980) 81.

[4] V. Perovic, G. R. Purdy, *et al.*, *Acta Metall.*, **29**:(1981) 889.

[5] V. Perovic, G. R. Purdy, *et al.*, *Scripta Metall.*, **15**(2):(1981) 217.

[6] J. M. Silcock, *Journal of the Institute of Metals*, **84**:(1955) 19.

[7] J. M. Silcock, *Journal of the Institute of Metals*, **84**:(1955) 23.

[8] J. M. Silcock, H. M. Flower, *Scripta Materialia*, **36**:(2002) 389.

[9] L. Bourgeois, J. F. Nie, *et al.*, *Philos. Mag.*, **85**(29).

[10] G. Bouvy, R. Graf, *C. R. Acad. Sci.*, **260**(18):(1965) 4742.

[11] J. M. Rosalie, L. Bourgeois, *et al.*, *Philos. Mag.*, **89**(25):(2009) 2195.

[12] G. Thomas, *Philos. Mag.*, **4**(48):(1959) 1213.

[13] K. H. Westmacott, R. L. Peck, *Philos. Mag.*, **23**(183):(1971) 611.

[14] D. E. Passoja, G. S. Ansell, *Acta Metall.*, **19**:(1971) 1253.

[15] G. R. Frank, Jr, D. Robinson, *et al.*, *J. Appl. Phys.*, **32**(9):(1961) 1763.

[16] R. B. Nicholson, J. Nutting, *Acta Metall.*, **9**:(1961) 332.

[17] D. Finkenstadt, D. D. Johnson, *Phys. Rev. B*, **73**(024101):(2006) 024101.